PERGAMON

Deep-Sea Research II 50 (2003) 925–950

DEEP-SEA RESEARCH
PART II

www.elsevier.com/locate/dsr2

Methane in ocean waters of the Bay of Bengal: its sources and exchange with the atmosphere

Ulrich Berner[a,*], Jürgen Poggenburg[a], Eckhard Faber[a], Detlef Quadfasel[b], Andrea Frische[c]

[a] *BGR, Federal Institute for Geosciences and Natural Resources, Stilleweg 2, D-300631 Hannover, Germany*
[b] *Niels Bohr Institute for Astronomy, Physics and Geophysics, University of Copenhagen, Juliane Maries Vej 30, 2100 Copenhagen, Denmark*
[c] *IfM, Institute of Oceanography, University of Hamburg, Troplowitzstraße 7, 22529 Hamburg, Germany*

Received 29 November 1999; accepted 12 September 2000

Abstract

Three legs of cruise SO93 of the German research vessel R/V SONNE provided information on the methane distribution along different profiles of the Bay of Bengal during the NE monsoon in January 1994. A 650-km-long profile from the Sri Lankan coast to the Equator revealed maximum methane concentrations clearly associated with different water masses. Peak concentrations of 105 nl/l occur below 45 m water depth. A 2600-km-long profile from the Equator to the shelf of Bangladesh showed elevated concentrations in the surface waters (up to 800 nl/l on the shelf close to the Ganges/Brahmaputra mouth). Waters at 700 and 2100 m off Bangladesh are enriched in methane. Seismic profiles of the Parasound system point to the existence of a mud diapir at 2100 m, and a seismic wipe out at 700 m points to gas-charged sediments. Sediment gases are assumed to be the source of the methane in the deep water of this area. However, no exchange with the surface waters was observed. Methane contents of the surface waters are related to bacterial processes as shown by isotope data of methane. This newly generated methane only partly contributes to the atmospheric methane concentrations, especially on the shelf of Bangladesh close to the Ganges/Brahmaputra mouth with flux rates of 145 kg km^{-2} year^{-1}. Large sections of the profiles, however, showed near-equilibrium conditions and even undersaturation of methane with respect to the atmosphere.

1. Introduction

Atmospheric water vapor and carbon dioxide, as they appear in larger quantities in the atmosphere, are unquestionably the major absorbers of radiative energy that build up the Earth's greenhouse (Graedel and Crutzen, 1993). Among other trace gases, like ozone, nitrous oxide, and chlorofluorocarbons, that add to the greenhouse-effect, methane plays a significant role and estimates of Houghton et al. (1990) suggest a contribution of 1.7 W m^{-2} from the present atmospheric methane concentration of 1.73 ppmV (parts per million, atmospheric mixing ratio).

*Corresponding author. Fax: +49-511-643-3664.
E-mail addresses: ulrich.berner@bgr.de (U. Berner), dq@gfy.ku.dk (D. Quadfasel), frische@ifm.uni-hamburg.de (A. Frische).

0967-0645/03/$ - see front matter
doi:10.1016/S0967-0645(02)00613-6

Although methane concentrations are small and the related present-day greenhouse effect seems to be low, compared the major constituents water vapor and carbon dioxide, quantifying even these minor contributions is essential for the understanding and modeling of climatic changes. Particularly since estimates by Houghton et al. (1990) suggest that methane has a 21-fold higher potential for global warming than an equal amount of carbon dioxide.

Methane concentrations have increased significantly during the last 200 years, from 0.7 to 1.73 ppmV, especially since 1930 (Rasmussen and Khalil, 1981; Houghton et al., 1990). However, the methane increases nearly stopped at the beginning of this decade for reasons not fully understood.

The increase in concentration relates partly to anthropogenic source; however, data form ice cores (Raynaud et al., 1988; Chappellaz, 1990; Chappellaz et al., 1990, 1993, 1997) show that we also must consider natural fluctuations as they have occurred during changes between glacial and interglacial times. In order to understand the natural variability of atmospheric methane concentrations, it is essential to determine the variability of the natural methane sources and sinks. One uncertainty concerning the global methane budget is the estimate of the global flux from the different sources, such as terrestrial and marine ecosystems, and the contribution of anthropogenic methane production (fossil fuel combustion, forest burning, cattle breeding, rice fields). Hein et al. (1997) have given a summary and demonstrated that methane flux into the atmosphere from different natural sources is highly variable. However, Hein et al. (1997) did not incorporate into their considerations the oceanic sources and sinks, as the uncertainties are high. According to Crutzen's (1991) estimates, total methane emissions amount to 640 Tg CH_4 per year, while Dlugokencky et al. (1998) calculated 549 Tg CH_4 per year on the basis of atmospheric measurements and Heimann (1997) reports a slightly higher value of 575 Tg CH_4 per year. Modeling of methane emissions amounts, depending on the scenario, to values between 562 and 592 Tg CH_4 per year, which shows that uncertainties on global methane emissions are still high and are in the order of the global atmospheric increases of more than 33 Tg CH_4 per year (Hein et al., 1997; Heimann, 1997).

Oceans and marine coastal areas are a potential source of methane and cannot be neglected for consideration of the global methane balance (Atkinson and Richards, 1967; Scranton and Farrington, 1977; Scranton and Brewer, 1977; Ward et al., 1987; Conrad and Seiler, 1988; Welhan, 1988; Owens et al., 1991; Bange et al., 1994; Faber et al., 1994; Faber et al., 1995; Bange et al., 1998a, b; Suess et al., 1998). Bange et al. (1998a, b) showed in their compilation (using data of Ericksson III, 1993 and Liss and Merlivat, 1986) that 10.9–17.8 Tg CH_4 are emitted from the world oceans per year, nearly half the atmospheric increase of 33.4 Tg CH_4 per year (Crutzen, 1991; Hein et al., 1997).

Besides being a source of methane, especially in coastal areas, the world oceans also represent a sink of this atmospheric trace gas (Faber et al., 1995), which is neglected in global methane balance considerations and modeling (Heimann, 1997; Hein et al., 1997; Dlugokencky et al., 1998) that relay largely on atmospheric hydroxyl-reactions and soil uptake as sinks for methane. Significant uncertainties about the amount of methane emitted and consumed by the oceans still exist, due to the high seasonality of methane emissions and also due to the unknown distribution and the patchiness of marine sources and sinks.

One of the objectives of cruise SO93 of the German research vessel R/V SONNE in January 1994 to investigate the potential of the Bay of Bengal as a source and/or sink for atmospheric methane. Three legs provided information from different areas of the Bay of Bengal not only on the methane concentrations in the water column and the atmospheric exchange, but also the possible exchanges between sediment and ocean waters. The intention of this paper is to give an overview of the methane inventory of the Bay of Bengal.

2. Oceanographic and regional geological setting

The Bay of Bengal comprises the NE part of the Indian Ocean (Fig. 1) and extends over a distance

of more than 2500 km between 22°N and the Equator. The water depth varies between 10 m in the shelf area of Bangladesh to more than 4500 m at the Equator. It represents the low-salinity portion of the northern Indian Ocean contrary to the high-salinity waters of the Arabian Sea. The low salinity of the surface waters of the Bay of Bengal is caused through the high river run-off of the Ganges/Brahmaputra (Fig. 5, Figs. 13–15) and also through the evaporation and precipitation conditions in the northern part of this area. The temperature distribution of the surface waters is also influenced through the river run-off (compare Fig. 4, Figs. 12–14). Oxygen minimum conditions within the water masses between the thermocline and 800 m (Fig. 6) are caused by bacterial consumption due to the oxidation of sinking particulate and dissolved organic compounds produced in the photic zone. Satellite images of the Bay of Bengal (Fig. 3) show that the highest pigment concentrations of phytoplankton occur at the shore lines. The surface waters of the open ocean are comparatively depleted. The average pigment concentration in the open ocean is on the order of $0.2\,mg\,m^{-3}$. The distribution and availability of organic compounds is coupled to the concentration of phyto- and zooplankton. In the sea surface and as well in oxygen-deficient waters of the deeper water body the formation of methane also can be related to bacterial activity under anoxic conditions in the interior of settling organic particles (phytoplankton, fecal pellets, etc.) or in the guts of zooplankton organisms (Oremland, 1993; Owens et al., 1991; Karl and Tilbrook, 1994). As the Bay of Bengal is a part of the northern Indian Ocean, the oceanic circulation is controlled through the seasonally changing monsoon gyre, which in turn toggles the concentration of nutrients and hence organic matter in the sea surface. The atmospheric circulation is also responsible for changing degassing and exchange rates between surface water and atmosphere with respect to volatile compounds.

The surface currents in the northern part of the Bay of Bengal show a strong north-east component during the NE monsoon of the north hemispheric winter months, while in the southern part the currents are typically in the east–west direction (Wyrtki, 1973). During the NE monsoon the current velocities south of Sri Lanka are the strongest of the whole Indian Ocean and may exceed 1 knot. According to Wyrtki (1973) a major branch of the low-salinity water of the Bay of Bengal is then transported into the eastern Arabian Sea. Under favorable wind conditions a weak upwelling may be possible at the eastern shore of the Andaman Sea.

During the SW monsoon (April–August) the surface circulation changes significantly. The currents of the southern Bay of Bengal are directed from west to east, which are again very strong south of Sri Lanka. The high-salinity waters of the Arabian Sea are transported through this current along the south coast of Sri Lanka. The salinity maximum formed within the thermocline of the Arabian Sea is only spread into the southernmost part of the Bay of Bengal (Fig. 5). But from this high-salinity layer, water proceeds to greater depth, and between 300 and 500 m high-salinity waters are spread with the SW monsoon to the west of Sumatra and into the Bay of Bengal (Fig. 5). The low-salinity surface water of the Bay of Bengal during the SW monsoon flows to the SE and along the coast of Sumatra. Under favorable conditions the SW monsoon may cause a weak upwelling along some parts of the eastern Indian coast.

The Bay of Bengal is by far the largest deep-sea fan of the earth. Its sedimentary infill is largely derived from the Himalayas transported through the Ganges–Brahmaputra Rivers into the northern Indian Ocean. The huge amount of erosional detritus is distributed into the ocean via turbidite currents. According to the ODP/DSDP drill sites 218 and 717 in the outer fan at a distance of more than 2000 km from the river mouth, about 75 m of predominantly mud turbidites were deposited during the last 465,000 years. Sediment thickness and consequently rate of accumulation significantly increase from the distal to the proximal part of the fan. High amounts of mainly terrestrial organic matter is spread and accumulated via these turbidites over the whole fan area and can be buried to sediment depths of more than 2000 m in the proximal part, close to the shelf. The organic carbon in the sediment is partly consumed and

converted via bacterial sulfate reduction to carbon dioxide, which can lead to a total depletion of pore water sulfate and which in turn enables methanogenic bacteria to convert carbon dioxide into methane. The sedimentary methane can be a source for the sea-water methane, provided suitable pathways for water and methane discharge are present in the sediments. This should likely be the case close to the shelf area as the delta is still subsiding and represents the tectonically active part of the fan.

3. Samples and methods

3.1. Water sampling and hydrographic measurements

Using a General Oceanics (USA) rosette water-sampler provided with 12 bottles, 370 ocean water samples were collected from various locations (Figs. 1 and 2) and depths of the Bay of Bengal. Additionally, oxygen concentrations, salinity, temperature and pressure were measured continuously in the water column with a SeaBird SBE11 plus CTD-probe mounted on the rack of the water-sampler, also equipped with three pairs of deep sea thermometers which were used for temperature calibrations. Oxygen concentrations measured with the CTD-sensor were calibrated by Winkler-titration during the cruise (Figs. 1–6).

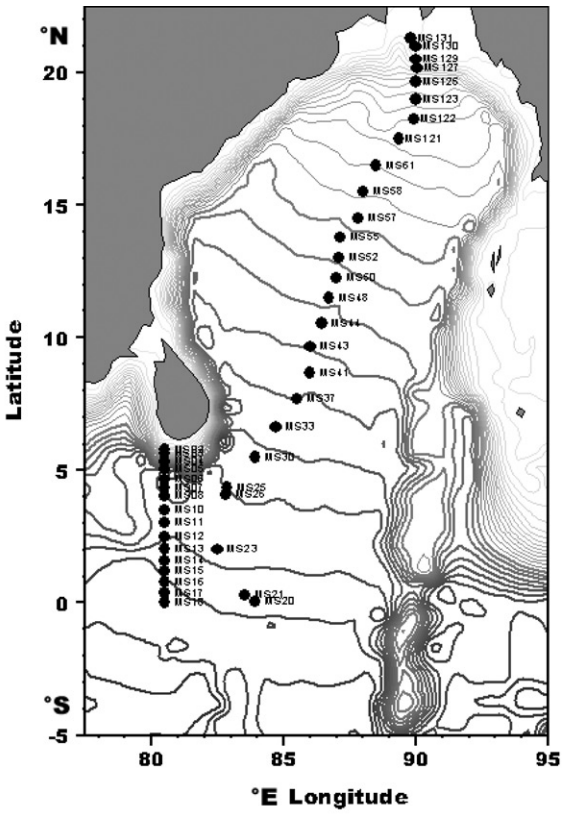

Fig. 1. The Bay of Bengal as part of the northern Indian Ocean. Positions of sample sites are marked by red circles together with site numbers of cruise SO93.

3.2. Methane measurements

After retrieval of the water-sampler bottles, the dissolved gases (containing oxygen, nitrogen, carbon dioxide, methane, and other trace gases) were subsequently extracted from the water samples by a vacuum/headspace technique (modified after Schmitt et al., 1991) aboard R/V "SONNE", and expanded via a needle valve into pre-evacuated glass bottles, sealed with a rubber septum and a metal crimp for shore-based isotope analyses. The rubber septum of each vial was again sealed with silicon rubber to ensure gas tight conditions. Two 0.5 ml aliquots of the total gas of each sample were injected into a Shimadzu GC Mini 3 gaschromatograph and analyzed for their methane concentrations. The gaschromatograph was provided with a flame ionization detector (FID), and a 2-m-long steel column, filled with Porapack Q. As reference for all measurements, atmospheric methane concentration of 1.7 ppm was used (Houghton et al., 1990). Methane concentrations are given as nl/l. The precision of the GC measurements at the concentration level of atmospheric methane is $\pm 15\%$, as determined from 1200 atmosphere samples. The accuracy of the methane determination in ocean water using the Schmitt et al. (1991) method is ± 5.8 nl/l. Tests by Schmitt et al. (1991) have shown that the recovery through the ultrasonic method is about 88% of the total dissolved methane. The methane concentrations given in our present paper are derived from a conversion of our data from

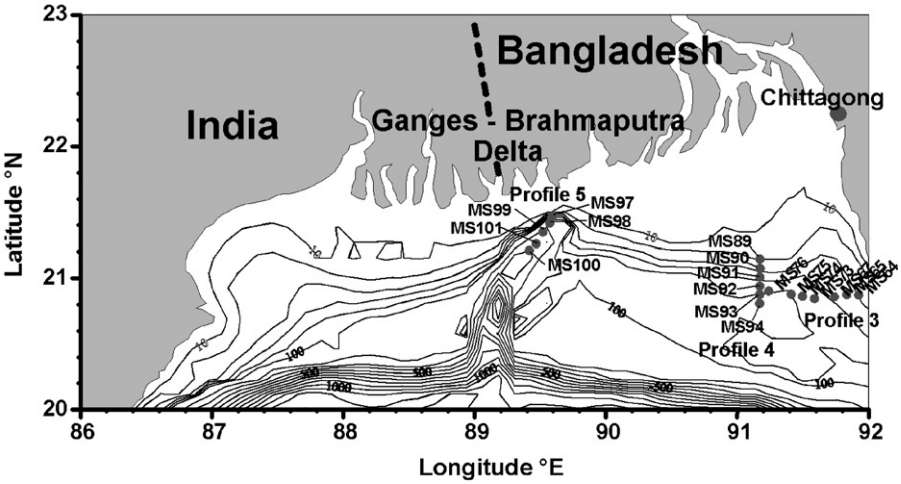

Fig. 2. The Ganges–Brahmaputra delta of the northern Bay of Bengal. Positions of shelf sites are marked by red circles together with the site numbers of cruise SO93.

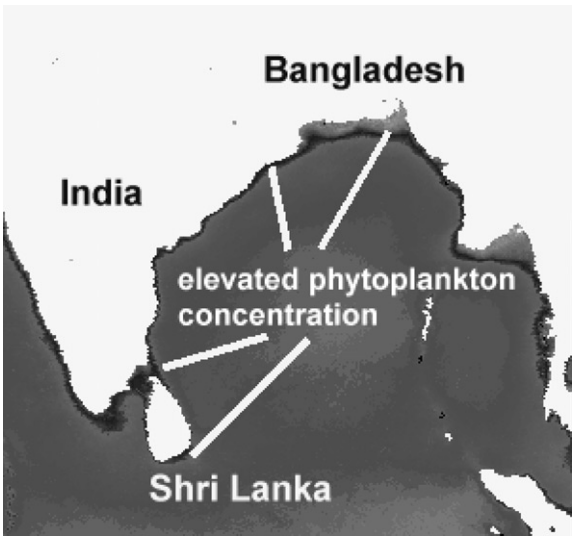

Fig. 3. Composite satellite image of the phytoplankton pigment distribution of surface waters of the western Bay of Bengal on December 29, 1985 (courtesy CRSA, USA).

ultrasonic treatment into absolute values based on a calibration study between different laboratories in Hamburg (Institute for Biogeochemistry and Marine Chemistry), Kiel (GEOMAR) and Hannover (BGR) (cf. Michaelis et al., 1993).

3.3. Methane flux calculations

The flux of gas from the sea surface to the atmosphere is controlled by wind speed, sea-surface temperature, and equilibrium conditions between sea and atmosphere. We calculate the sea–air flux of methane F from the equation of Wanninkhof (1992)

$$F = \frac{0.31 v^2 \Delta C}{\sqrt{\frac{2039.2 - 120.31 T_C + 3.4209 T_C^2 - 0.040437 T_C^3}{660}}} \quad (1)$$

where v is the wind speed (m/s), T_C is the sea-surface temperature in °C, and ΔC is the difference between measured concentrations and equilibrium solubility of methane. Wind speed and sea-surface temperature were monitored routinely during the cruise. Equilibrium solubilities C (nl/l) that are related to sea surface temperature and salinity were computed from the equation of Wiesenburg and Guinasso (1979)

$$\ln C = \ln f_G - 412.171 + 596.8104\left(\frac{100}{T}\right) + 379.2599 \ln\left(\frac{T}{100}\right) - 62.0757\left(\frac{T}{100}\right)$$

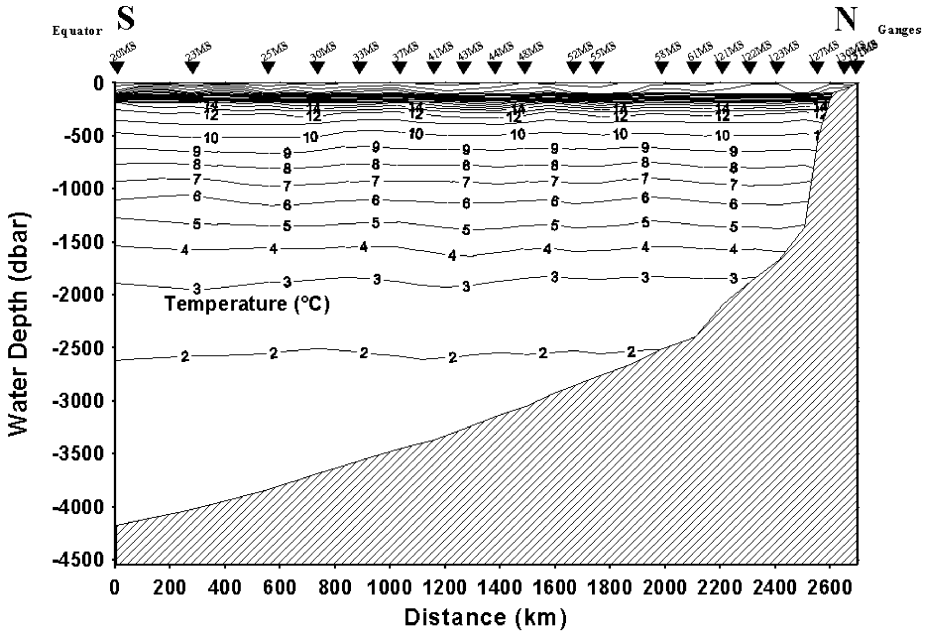

Fig. 4. Temperature distribution of waters of the Bay of Bengal. Positions of sites are marked by triangles together with site numbers of cruise SO93 (Profile 2).

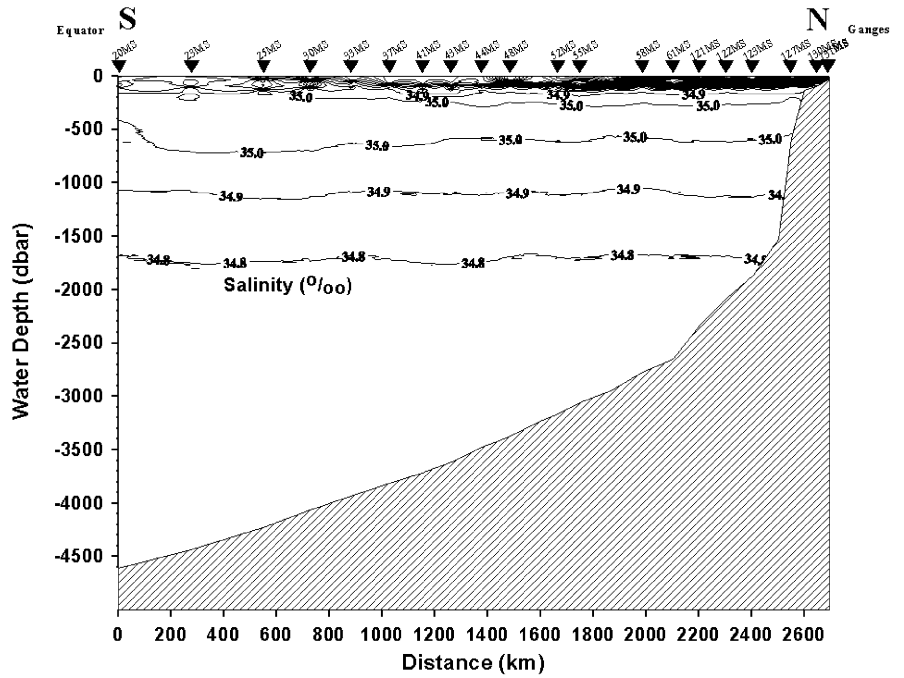

Fig. 5. Salinity distribution of waters of the Bay of Bengal. Positions of sites are marked by triangles together with site numbers of cruise SO93 (Profile 2).

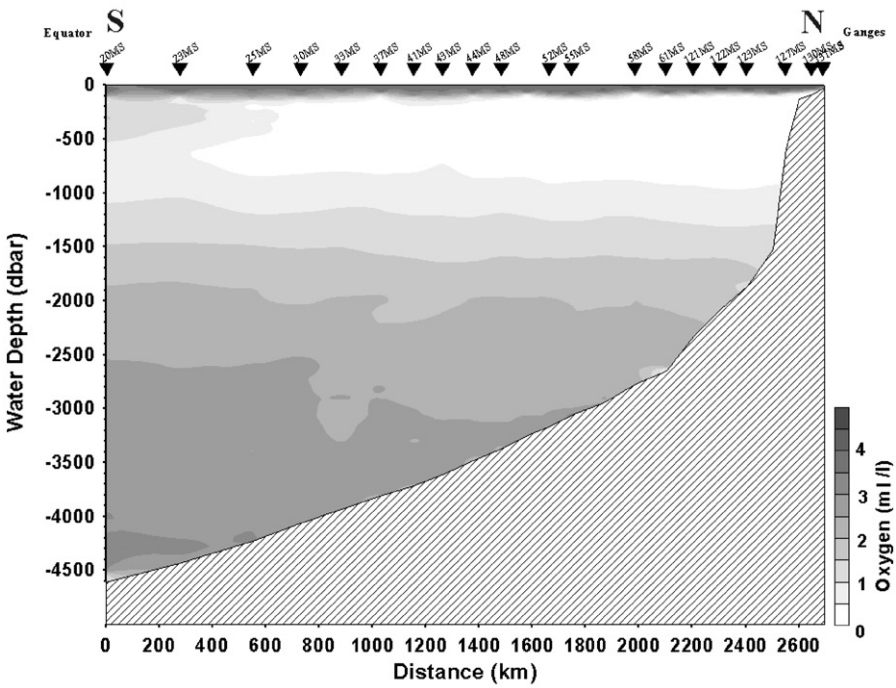

Fig. 6. Oxygen distribution of waters of the Bay of Bengal. Positions of sample sites are marked by triangles together with site numbers of cruise SO93 (Profile 2).

$$+ S\left[-0.059160 + 0.032174\left(\frac{T}{100}\right) - 0.0048198\left(\frac{T}{100}\right)^2\right], \quad (2)$$

where f_G is the atmospheric concentration of methane that we assume to be represented in the Bengal Bay by an average atmospheric methane concentration of 1.73 ppmV (Houghton et al., 1990; Graedel and Crutzen, 1993), T is sea surface temperature in K, and S is salinity in ‰. All estimates of methane-flux F were converted into kg km^{-2} yr^{-1} to be comparable to values given in the literature.

3.4. Carbon isotopic measurements

Carbon isotope ratios of methane were analyzed with a *g*as-*c*hromatograph *i*sotope *r*atio *m*ass *s*pectrometer (GC-IR-MS). The system is based on a Finnigan MAT 252 mass spectrometer that was combined with a gas chromatograph for separation of individual gas components and a combustion oven to convert methane into carbon dioxide. The gas-separation system was designed at the laboratory of the BGR. The combustion CO_2 is flushed separately with He via a split system into the ion source of the mass spectrometer. Carbon isotope ratios of methane are given as δ^{13}C-values relative to the PDB standard. The amount of methane required for analysis is below 5 nl. Reproducibility (1σ) of δ-values (tested by repeated injection of 2 ml of air) is about ± 1‰. Further information on the isotope technique is given in Faber et al. (1994, 1998).

Methane concentrations, methane fluxes and carbon isotope ratios of methane of water samples are given in Tables 1–3.

4. Results and discussion

4.1. Region 1: Sri Lanka South

During the first leg of cruise SO93 the hydrographic programme concentrated on a profile

Table 1
Sample sites of the southern Bay of Bengal offshore Shri Lanka (Profile 1, Cruise SO93)

Profile no.	Site position longitude east	Lattitude north	Windspeed (m/s)	Sample no.	Water depth (m)	Temperature (°C)	Salinity (‰)	Méthane (nl/l)	Methane flux rate ($kg\,km^{-2}\,yr^{-1}$)
1	80.485	5.636	0.8	03-MS#12	10	27.0	33.1	73	0.35
				03-MS#11	50			52	
				03-MS#9	100			109	
1	80.493	5.336	0.9	04-MS#12	10	27.7	34.1	55	0.17
				04-MS#11	50			63	
				04-MS#10	100			79	
				04-MS#9	150			78	
1	80.491	5.036		05-MS#11	50			60	
				05-MS#10	100			76	
				05-MS#9	125			59	
1	80.497	4.670	4.8	06-MS#12	10	28.3	35.4	48	1.69
				06-MS#11	50			56	
				06-MS#10	100			78	
				06-MS#9	125			56	
1	80.498	4.040	8.4	08-MS#12	10	28.1	35.4	38	−9.98
				08-MS#11	50			68	
				08-MS#10	100			70	
				08-MS#9	125			96	
1	80.496	3.497	3.9	10-MS#12	10	28.1	35.4	37	−2.39
				10-MS#11	50			71	
				10-MS#10	100			59	
				10-MS#9	125			60	
1	80.499	2.031	2.1	13-MS#12	10	28.2	35.2	39	−0.48
				13-MS#11	50			35	
				13-MS#10	100			46	
				13-MS#9	125			39	
1	80.493	1.579	6.2	14-MS#12	10	28.1	35.2	32	−9.52
				14-MS#10	100			44	
				14-MS#9	125			58	
1	80.503	1.186	5.0	15-MS#12	10	28.3	35.0	37	−3.65
				15-MS#11	50			97	
				15-MS#10	100			93	
				15-MS#9	125			56	
1	80.499	0.030	3.7	18-MS#12	10	28.4	35.2	32	−3.47
				18-MS#11	50			65	
				18-MS#10	100			51	
				18-MS#9	125			34	

Table 2
Sample sites of the Bay of Bengal (Profile 2, Cruise SO93)

Profile	Site position longitude east	Latitude north	Windspeed (m/s)	Sample no.	Water depth (m)	Temperature (°C)	Salinity (‰)	CH_4 (nl/l)	CH_4 $\delta^{13}C$ (‰)	CH_4 flux rate (kg km^{-2} yr^{-1})
2	83.920	0.045	5.1	20-MS#10	10	28.7	35.1	75	−45.5	−0.38
				20-MS#9	100			58		
				20-MS#8	125			85	−38.4	
				20-MS#7	500			48		
				20-MS#6	1000			96	−26.4	
				20-MS#5	2000			47	−25.7	
				20-MS#4	3000			9		
				20-MS#2	4511			133		
				20-MS#1	4606			35	−31.4	
2	82.497	2.008	2.5	23-MS#12	10	28.6	35.2	67	−46.1	0.84
				23-MS#11	50			102	−39.5	
				23-MS#10	100			84	−39.7	
				23-MS#9	125			29		
				23-MS#8	500			25		
				23-MS#7	1000			110	−27.3	
				23-MS#6	2000			74	−31.1	
				23-MS#5	3000			28		
				23-MS#4	4001			12		
				23-MS#3	4331			30		
				23-MS#2	4390			37		
				23-MS#1	4435			34		
2	82.869	4.339	1.2	25-MS#11	10	28.6	34.8	100	−42.6	0.97
				25-MS#10	50			72	−45.1	
				25-MS#9	100			78	−46.9	
				25-MS#8	125			51		
				25-MS#7	500			65		
				25-MS#6	1000			28	−30.2	
				25-MS#5	2000			19		
				25-MS#4	3000			18		
				25-MS#3	4000			24		
				25-MS#2	4141			38		
				25-MS#1	4186			16		
				25-MS#12	4233			2		
2	83.914	5.501	7.9	30-MS#12	10	28.4	34.5	57		−1.65
				30-MS#11	50			170		
				30-MS#10	100			70		
				30-MS#9	125			109		

Table 2 (*continued*)

Profile	Site position longitude east	Latitude north	Windspeed (m/s)	Sample no.	Water depth (m)	Temperature	Salinity (‰)	CH_4 (nl/l)	CH_4 $\delta^{13}C$ (‰)	CH_4 flux rate ($kg\,km^{-2}\,yr^{-1}$)
				30-MS#7	1001			34		
				30-MS#6	2200			48		
				30-MS#5	2850			10		
				30-MS#4	3301			20		
				30-MS#3	3965			21		
				30-MS#2	4012			20		
				30-MS#1	4064			14		
2	84.703	6.631	9.2	33-MS#12	10	27.9	34.4	41		−24.57
				33-MS#11	50			65	−39.4	
				33-MS#10	100			60	−44.0	
				33-MS#9	125			90	−46.0	
				33-MS#8	500			37	−27.6	
				33-MS#7	999			33		
				33-MS#6	2001			22		
				33-MS#5	3000			17		
				33-MS#4	3500			11		
				33-MS#3	3832			20		
				33-MS#2	3882			37	−34.3	
				33-MS#1	3937			23	−43.0	
2	85.500	7.671	7.9	37-MS#12	10	27.8	34.2	40		−6.07
				37-MS#ll	50			126	−46.5	
				37-MS#10	100			64	−41.8	
				37-MS#9	125			33		
				37-MS#8	251			32	−30.4	
				37-MS#7	1000			8		
				37-MS#6	2000			19		
				37-MS#5	3000			9		
				37-MS#4	3715			18		
				37-MS#3	3767			16		
				37-MS#2	3812			22	−39.1	
2	85.991	8.673	8.6	41-MS#12	10	28.4	34.2	48		5.35
				41-MS#11	50			63		
				41-MS#10	100			64		
				41-MS#9	125			101		
				41-MS#8	250			57		
				41-MS#7	500			23		
				41-MS#6	1000			15		
				41-MS#5	2000			9		

				41-MS#4	3001			11			
				41-MS#3	3619			10			
				41-MS#2	3662			25			
				41-MS#1	3715			13			
2	86.000	9.667	5.4	43-MS#12	10	28.3	34.2	26	−46.3	−11.50	
				43-MS#11	50			50	−43.9		
				43-MS#10	101			80	−47.4		
				43-MS#9	125			94	−42.5		
				43-MS#8	250			54	−38.4		
				43-MS#7	500			28	−29.5		
				43-MS#6	1000			17			
				43-MS#5	2000			2			
				43-MS#3	3517			13			
				43-MS#2	3568			19			
				43-MS#1							
2	86.434	10.532	5.9	44-MS#12	10	28.0	34.2	49		3.20	
				44-MS#11	50			88			
				44-MS#10	101			92			
				44-MS#9	125			96			
				44-MS#8	250			54			
				44-MS#7	500			27			
				44-MS#6	1005			13			
				44-MS#5	2000			8			
				44-MS#3	3382			8			
				44-MS#2	3445			31			
				44-MS#1	3478			11			
2	86.700	11.500	4.8	48-MS#11	10	26.9	33.2	77	−40.2	14.33	
				48-MS#10	50			46	−46.4		
				48-MS#9	100			94	−48.1		
				48-MS#8	125			34	−36.0		
				48-MS#7	250			16	−36.8		
				48-MS#6	500			6			
				48-MS#5	1000			32			
				48-MS#4	2000			27			
				48-MS#3	3000			13			
2	87.000	12.251		50-MS#11	50			56			
				50-MS#10	101			138			
				50-MS#9	125			83			
				50-MS#8	250			31			
				50-MS#7	500			20			
				50-MS#6	1000			14			
				50-MS#5	2001			7			

Table 2 (*continued*)

Profile	Site position longitude east	Latitude north	Windspeed (m/s)	Sample no.	Water depth (m)	Temperature	Salinity (‰)	CH_4 (nl/l)	CH_4 $\delta^{13}C$ (‰)	CH_4 flux rate (kg km^{-2} yr^{-1})
				50-MS#4	3001			4		
				50-MS#3	3154			7		
				50-MS#2	3206			9		
				50-MS#1	3250			7		
2	87.098	13.004	1.2	52-MS#12	10	27.4	33.5	46		0.02
				52-MS#11	49			63	−44.5	
				52-MS#10	102			78	−45.7	
				52-MS#9	126			112	−44.8	
				52-MS#8	249			40	−40.6	
				52-MS#7	500			20	−38.2	
				52-MS#6	1000			8	−39.4	
				52-MS#5	2000			11		
				52-MS#4	2500			3		
				52-MS#3	3066			5		
				52-MS#2	3114			19		
				52-MS#1	3159			5	−39.9	
2	87.120	13.782	3.6	55-MS#12	10	27.2	33.1	40		−1.54
				55-MS#11	50			49		
				55-MS#10	100			93		
				55-MS#9	125			75		
				55-MS#8	250			27		
				55-MS#7	500			16		
				55-MS#5	2000			3		
				55-MS#4	2500			2		
				55-MS#3	2963			3		
				55-MS#2	3014			10		
				55-MS#1	3059			2		
2	87.820	14.504	5.5	57-MS#12	11	26.9	32.8	41	−40.1	−2.91
				57-MS#11	50			64	−42.1	
				57-MS#10	100			113	−43.8	
				57-MS#9	125			85	−45.8	
				57-MS#8	250			35	−40.1	
				57-MS#7	500			19	−40.7	
				57-MS#6	1001			14	−39.5	
				57-MS#5	2000			8		
				57-MS#4	2501			9		
				57-MS#3	2847			11		
				57-MS#2	2895			19		
				57-MS#1	2942			10	−35.4	

2	88.001	15.518	2.7	58-MS#12	10	26.1	31.6	57		1.41	
				58-MS#11	50			71			
				58-MS#10	101			125			
				58-MS#9	123			81			
				58-MS#8	250			21			
				58-MS#7	500			17			
				58-MS#6	1000			15			
				58-MS#5	2000			3			
				58-MS#4	2500			6			
				58-MS#3	2680			5			
				58-MS#2	2730			1			
				58-MS#1	2775			6			
2	88.497	16.501	5.9	61-MS#12	10	26.1	32.7	39	−40.1	−5.10	
				61-MS#11	50			62	−38.7		
				61-MS#10	100			141	−43.3		
				61-MS#9	125			82	−40.2		
				61-MS#8	250			34	−33.7		
				61-MS#7	500			18	−35.5		
				61-MS#6	1001			8	−34.5		
				61-MS#5	2001			10			
				61-MS#4	2500			9			
				61-MS#3	2555			8			
				61-MS#2	2605			19			
				61-MS#1	2651			4	−37.6		
2	89.364	17.503	6.0	121-MS#12	10	26.0	32.1	55	−42.8	5.59	
				121-MS#11	50			90	−42.1		
				121-MS#10	100			77	−46.8		
				121-MS#9	125			58	−44.3		
				121-MS#7	250			22	−34.7		
				121-MS#5	1000			20	−32.2		
				121-MS#4	2000			33	−41.1		
				121-MS#1	2319			43	−42.1		
2	89.916	18.252	4.8	122-MS#12	10	25.1	30.4	67	−43.8	8.48	
				122-MS#11	75			92	−49.1		
				122-MS#10	100			57	−44.9		
				122-MS#9	125			41	−41.1		
				122-MS#7	250			12	−40.2		
				122-MS#5	1000			20	−40.6		
				122-MS#3	2000			62	−46.4		
				122-MS#1	2081			52	−43.7		
2	90.002	19.002	6.7	123-MS#12	10	25.0	29.8	80	−43.8	27.53	
				123-MS#11	50			117	−47.0		

Table 2 (*continued*)

Profile	Site position longitude east	Latitude north	Windspeed (m/s)	Sample no.	Water depth (m)	Temperature	Salinity (‰)	CH_4 (nl/l)	CH_4 $\delta^{13}C$ (‰)	CH_4 flux rate ($kg\,km^{-2}\,yr^{-1}$)
				123-MS#10	75			146	−57.2	
				123-MS#9	101			102	−45.1	
				123-MS#8	124			106	−46.2	
				123-MS#6	502			29	−31.9	
				123-MS#5	1000			41	−41.0	
				123-MS#4	1501			10	−41.3	
				123-MS#3	1768			18	−37.8	
				123-MS#1	1863			31	−37.2	
2	90.002	19.667	1.8	125-MS#12	11	26.1	32.3	92	−46.5	2.92
				125-MS#11	51			91	−41.2	
				125-MS#10	75			60	−45.3	
				125-MS#9	101			74	−51.8	
				125-MS#7	249			26	−38.4	
				125-MS#5	500			12	−40.2	
				125-MS#3	1427			23	−37.9	
				125-MS#1	1523			34	−41.7	
2	90.049	20.169	3.3	127-MS#9	10	25.2	30.1	87	−45.3	8.37
				127-MS#8	50			117	−48.7	
				127-MS#7	75			62	−44.8	
				127-MS#6	100			38	−46.3	
				127-MS#5	125			140	−58.6	
				127-MS#4	250			32	−49.2	
				127-MS#3	489			63	−48.9	
				127-MS#1	584			101	−49.6	
2	89.998	20.498		129-MS#6	30			83	−46.0	
				129-MS#5	50			100	−52.1	
				129-MS#4	75			85	−54.5	
				129-MS#3	100			81	−52.7	
				129-MS#2	130			71	−39.6	
2	90.002	21.001	1.7	130-MS#5	10	25.4	30.9	71	−45.6	1.33
				130-MS#4	30			64	−44.4	
				130-MS#3	50			82	−49.8	
				130-MS#1	87			77	−48.2	
2	89.800	21.301	2.8	131-MS#4	5	25.6	31.3	96	−54.5	7.48
				131-MS#3	10			100	−53.7	
				131-MS#1	25			252	−61.2	

Table 3
Sample sites of the northern Bay of Bengal (Bengal Shelf) offshore Bangladesh (Profiles 3 to 5, Cruise SO93)

Profile no.	Site position longitude east	Latitude north	Windspeed (m/s)	Sample no.	Water depth (m)	Temperature (°C)	Salinity (‰)	Methane (nl/l)	Methane flux rate ($kg\,km^{-2}\,yr^{-1}$)
3	91.935	20.864	10.1	64-MS#9	4	24.7	30.4	102	106.28
				64-MS#7	10			83	
				64-MS#5	21			211	
				64-MS#3	30			197	
				64-MS#1	33			232	
3	91.845	20.867	10.1	65-MS#6	6	25.4	30.9	120	145.39
				65-MS#5	10			79	
				65-MS#4	20			156	
				65-MS#3	30			232	
				65-MS#2	40			399	
				65-MS#1	42			360	
3	91.751	20.850	7.9	67-MS#7	5	24.6	30.2	96	56.92
				67-MS#6	10			111	
				67-MS#5	20			115	
				67-MS#4	30			200	
				67-MS#3	40			345	
				67-MS#2	50			418	
				67-MS#1	59			378	
3	91.600	20.837	4.9	73-MS#8	5	24.9	30.2	107	27.29
				73-MS#7	10			87	
				73-MS#6	20			287	
				73-MS#5	30			212	
				73-MS#4	40			152	
				73-MS#3	50			210	
				73-MS#2	60			216	
				73-MS#1	66			185	
3	91.509	20.854	4.9	74-MS#8	5	24.6	30.0	118	31.96
				74-MS#7	10			152	
				74-MS#6	20			178	
				74-MS#5	30			288	
				74-MS#4	40			389	
				74-MS#3	50			310	
				74-MS#2	60			201	
				74-MS#1	70			155	
3	91.251	20.894	5.3	76-MS#8	5	24.6	29.6	90	22.50

Table 3 (*continued*)

Profile no.	Site position longitude east	Latitude north	Windspeed (m/s)	Sample no.	Water depth (m)	Temperature (°C)	Salinity (‰)	Methane (nl/l)	Methane flux rate ($kg\,km^{-2}\,yr^{-1}$)
				76-MS#7	10			114	
				76-MS#6	20			648	
				76-MS#4	40			255	
				76-MS#3	50			171	
				76-MS#2	60			134	
				76-MS#1	74			120	
4	91.184	21.137	2.9	89-MS#3	6	19.7	27.3	118	9.45
				89-MS#2	10			206	
				89-MS#1	20			281	
4	91.187	21.066	2.9	90-MS#3	10	25.9	33.1	134	14.49
				90-MS#1	26			311	
4	91.184	21.002	2.9	91-MS#6	6	24.9	30.2	72	3.96
				91-MS#5	10			43	
				91-MS#4	20			64	
				91-MS#3	30			207	
				91-MS#2	40			134	
				91-MS#1	48			151	
4	91.181	20.866	2.9	93-MS#8	6	25.1	30.2	71	3.81
				93-MS#7	10			55	
				93-MS#6	21			105	
				93-MS#5	31			105	
				93-MS#4	40			172	
				93-MS#3	50			242	
				93-MS#2	60			226	
				93-MS#1	73			210	
4	91.183	20.799	6.0	94-MS#8	6	25.5	305	86	26.98
				94-MS#7	10			68	
				94-MS#6	21			69	
				94-MS#5	31			91	
				94-MS#4	40			204	
				94-MS#3	50			142	
				94-MS#2	60			131	
				94-MS#1	78			290	

5	89.606	21.442	2.4	97-MS#5	5	24.5	30.1	858	89.61
				97-MS#3	20			836	
				97-MS#1	40			573	
5	89.580	21.399		98-MS#4	100			105	
				98-MS#3	125			127	
				98-MS#2	150			102	
				98-MS#1	164			116	
5	89.459	21.241	0.8	100-MS#12	10	25.0	30.5	135	1.08
				100-MS#11	30			420	
				100-MS#10	50			216	
				100-MS#9	100			149	
				100-MS#7	200			123	
				100-MS#5	300			81	
				100-MS#3	400			84	
				100-MS#1	448			73	
5	89.410	21.167	2.4	101-MS#12	10	24.9	30.5	87	4.40
				101-MS#11	30			241	
				101-MS#10	50			211	
				101-MS#9	100			823	
				101-MS#8	200			170	
				101-MS#7	300			87	

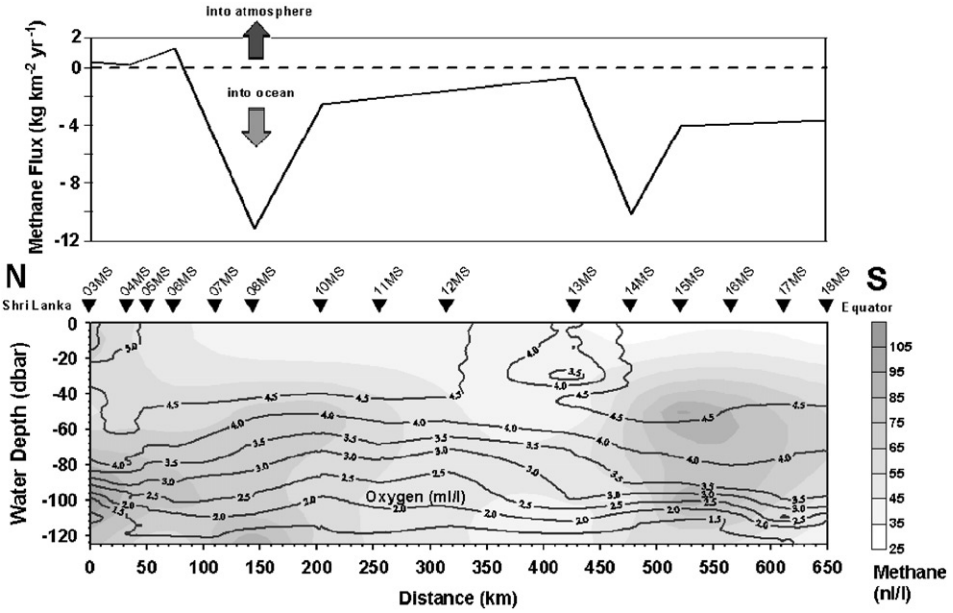

Fig. 7. Methane concentrations south of Sri Lanka are low and close to or below atmospheric equilibrium. Insignificant transport into the atmosphere is only observed in the northern part of the profile (Profile 1).

between the southern tip of Sri Lanka and the Equator along 80°30′E (compare Figs. 1 and 7) consisting of 15 stations (03MS to 18MS from N to S; Profile 1). Methane measurements were made to a maximum of 120-m water depth, whereas normal hydrographic investigations were carried out down to 1100 m.

The atmospheric circulation during the cruise as well as the distribution of temperature and salinity were typical for the NE monsoon. Low-salinity waters originating from the Bay of Bengal were found near the southern coast of Sri Lanka and high-salinity waters of western origin farther south. The two water masses were separated at about 300 km off the Sri Lankan coast (Fig. 7).

Maxima of methane concentrations are clearly associated with the different water masses observed off Sri Lanka. Peak concentrations of 105 nl/l occur below 45 m water depth. The likely source of methane in the oxygen-rich surface waters south off Sri Lanka are methanogenic bacteria which might either be associated with organic detritus or live in the guts of the zooplankton.

However, concentrations of surface waters (10 m) are largely below equilibrium with values below 45 nl/l. Only within the northern 100 km of the profile surface waters show methane concentrations slightly above the atmospheric equilibrium. Flux calculations (Eqs. (1) and (2)) employing measured wind speeds, temperatures and salinities result in low flux rates, with a maximum of 1.3 kg km^{-2} yr^{-1} for the northern part of the profile (Fig. 7). The low flux transports insignificant amounts of methane into the air as the rates are very close to equilibrium conditions whereas the majority of the surface waters represent a sink for atmospheric methane. Overall, this area south off Sri Lanka must be regarded as a sink for atmospheric methane, at least during the time of our measurements.

4.2. Region 2: equator to Bangladesh shelf

During the second leg of cruise SO93, a 2600-km-long S–N-profile (compare Fig. 1 and 8; Profile 2) from the Equator to the shelf area of Bangladesh was investigated. Although the atmospheric circulation was typical for the NE monsoon, the surface currents were highly variable throughout this leg and did not show a

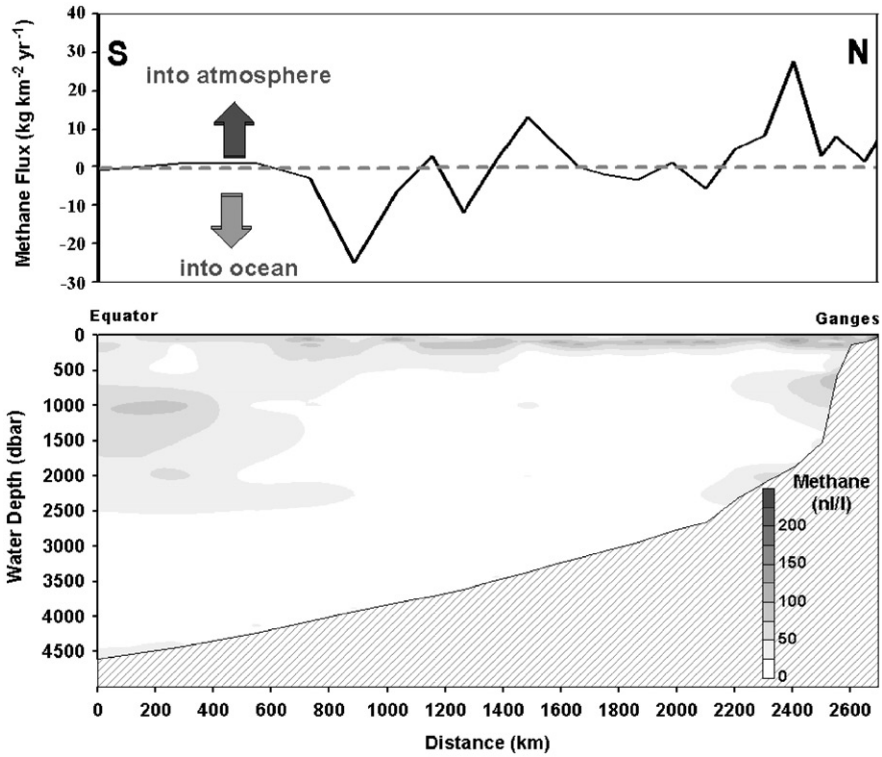

Fig. 8. Methane concentrations and exchange with the atmosphere in the Bay of Bengal (Profile 2).

well-defined pattern, indicating that transient eddy motion dominated the flow field.

The distribution of temperature and salinity shows strong horizontal gradients in the upper layer due to the influx of freshwater into the northern Bay of Bengal (Figs. 4 and 5). The thermocline varies around 100 m. The shallow (100 m) salinity maximum of the Subtropical Water penetrates only to about 7°N (33MS). The intermediate and deep layers are ventilated from the south with Central Water and Antarctic Bottom Water. An oxygen minimum (Fig. 6) extends from the shelf to about 4°N (25MS). The thickness of the oxygen minimum layer decreases from the shelf (80–900 m) towards the open Bay of Bengal (150–800 m).

Generally, deep waters show low concentrations of methane (Fig. 8) with the exception of the southern intermediate waters (20MS, 23MS, 25MS). Highest values are usually observed above the oxygen minimum zone between 125 and 2 m (compare Figs. 6, 8 and 12). Exceptions are found in the northern part of the profile (125MS, 127MS, 129MS) where high methane concentrations are associated with the oxygen minimum. The surface waters contained elevated methane concentrations, and maximum values of up to 220 nl/l were observed at the shelf edge of Bangladesh (Figs. 8 and 12).

Waters at the continental slope off Bangladesh at around 700 m and also at 2100 m were enriched in methane. Seismic profiles of the Parasound system (University of Bremen, Germany) show at 2100 m water depth the occurrence of a mud diapir (Fig. 9). It seems likely that at 700 and 2100 m gases are seeping from these sediments and they have contributed to the anomalous methane concentrations at these water depths. However, the gases do not reach the surface waters and hence do not contribute to the atmospheric methane concentrations.

The general increase of methane concentrations from sea floor to sea surface (Fig. 8) suggests that

methane flux from the sediments into the water column is of no importance (with the two described exceptions), and that in situ production within the water column must be responsible for the observed concentrations. The most likely process responsible for the methane anomalies in oxygen-rich waters is bacterial methanogenesis associated either with the decay of settling organic debris (from phyto- and zooplankton) or with gut bacteria within zooplankton.

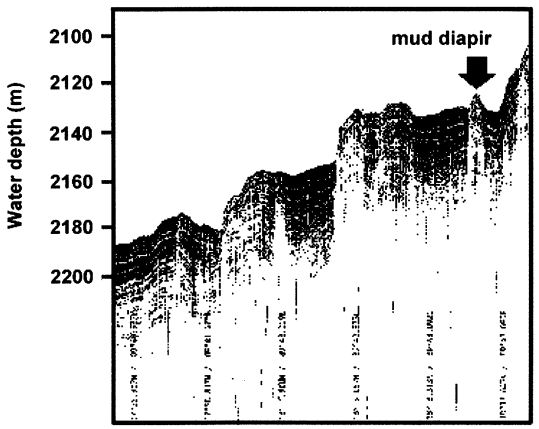

Fig. 9. A mud diapir is observed at 2100 m water depth where elevated methane concentrations are measured in the water column.

Carbon isotope ratios of methane in the sea surface show a range from −62 to −38‰. The light isotope values support the assumption that methane has been produced from bacterial methanogenic processes (Whiticar et al., 1986) within the oxygen-rich surface waters (Fig. 10), whereas the more positive values might be related to bacterial oxidation (Whiticar and Faber, 1986) where initially isotopic light methane is consumed and the residual methane is enriched in ^{13}C. The resulting carbon isotope ratio of the residual methane depends on the ratio of new production and the subsequent bacterial oxidation, and likely is toggled through ecological conditions in the waters.

The methane samples from the Bay of Bengal show a clear dependency on the degree of bacterial

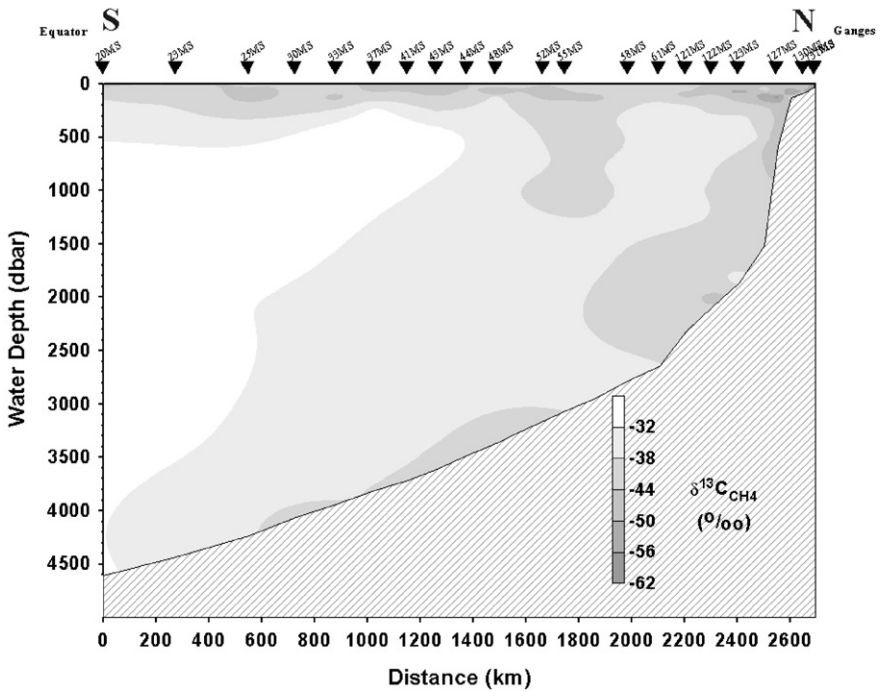

Fig. 10. Carbon isotope ratios of methane point to bacterial generation in surface waters of the Bay of Bengal (Profile 2).

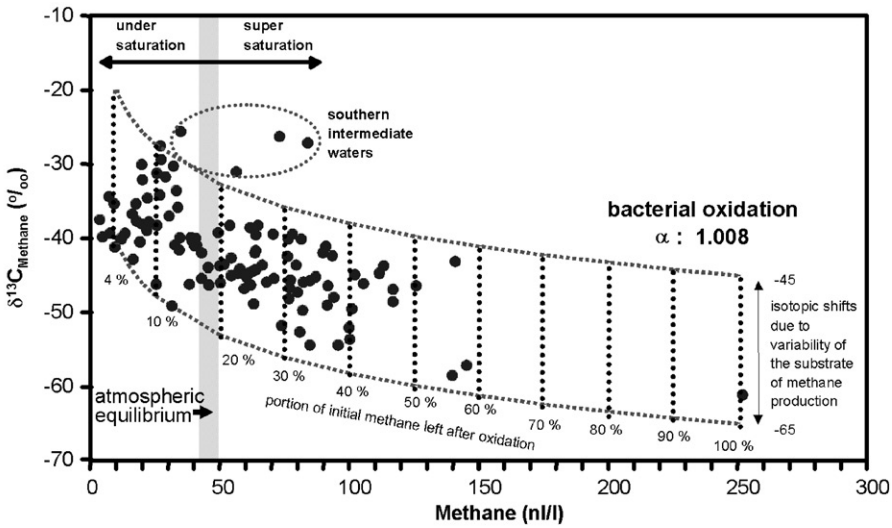

Fig. 11. Methane concentrations decrease and carbon isotope ratios of methane are shifted towards more positive values due to bacterial oxidation. Fields of super- and undersaturation with respect to atmospheric equilibrium are used to classify samples.

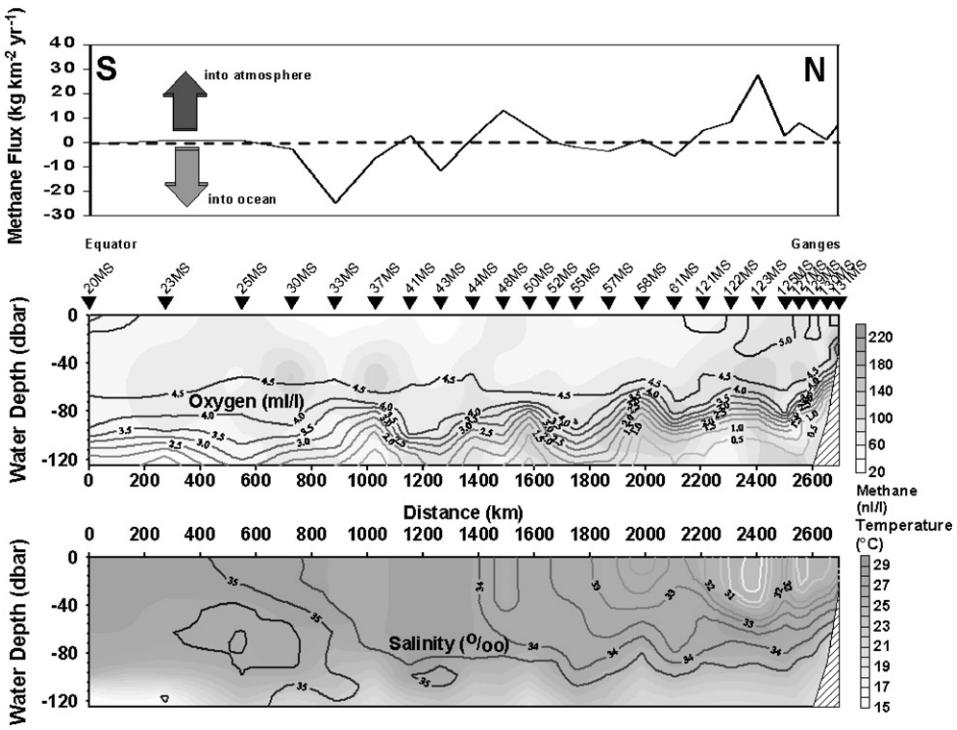

Fig. 12. Methane and oxygen concentrations, water temperatures, salinity and calculated methane flux in surface waters of the Bay of Bengal. Surface waters act as both a source and sink for atmospheric methane (Profile 2).

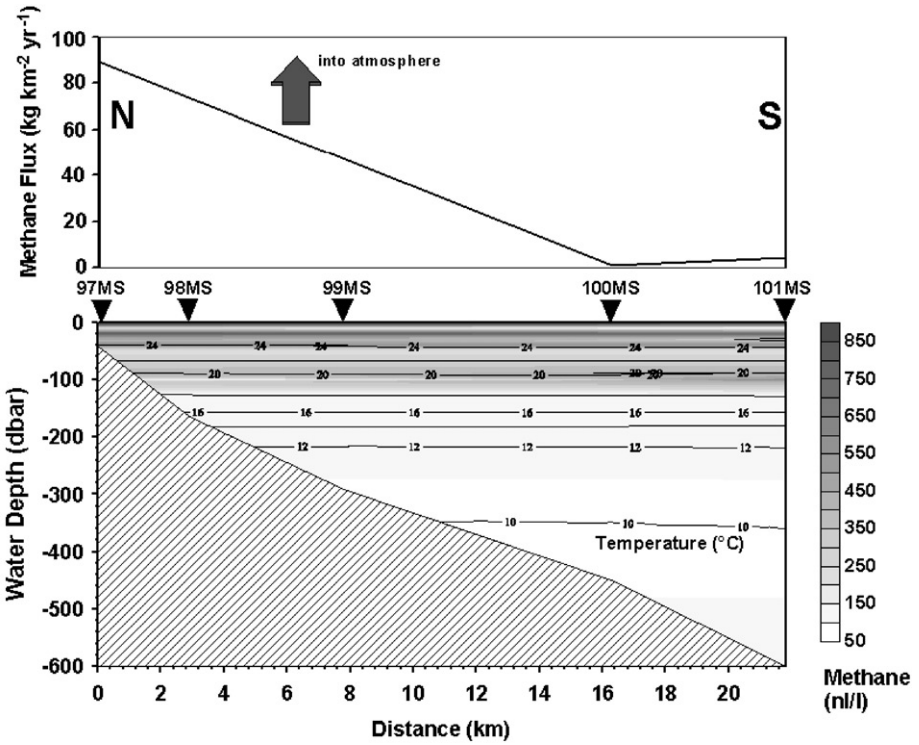

Fig. 13. Methane and oxygen concentrations, water temperatures and salinity of the eastern shelf of Bangladesh (E–W profile) and calculated methane flux rates (Profile 3).

oxidation they underwent. With decreasing methane concentrations as a result of decreasing production/oxidation ratios, the heavy carbon isotope is enriched in the residual methane fraction (Fig. 11). If we consider oxidation as the dominant process, then the isotopic shift (Fig. 11) with decreasing concentrations can best be described through a Rayleigh function with a fractionation factor of $\alpha = 1.008$, which is compatible with the findings of Faber et al. (1998) for oxidation processes in the surface waters of the Red Sea. The calculated oxidation trend assuming $\alpha = 1.008$ would be the same for lower initial concentrations. The isotopic variability of methane reaches 20‰ within this trend and likely represents the isotopic variability of the substrate on which methanogenic bacteria live.

However, the four samples from the intermediate waters at the two southern-most stations (MS20 and MS23) do not plot within the proposed oxidation trend but are shifted to more positive values (Fig. 11). This shift can be explained either by oxidative fractionation with a fractionation factor of $\alpha = 1.008$ and a high initial methane concentration of about 800 nl/l or alternatively by assuming a higher fractionation factor of $\alpha = 1.020$ for the bacterial oxidation process, implying an initial methane concentration at around 250 nl/l.

Despite the fact that methane is at least partly consumed in the surface waters, our investigations show that the ocean waters of the Bay of Bengal can be regarded as a minor source, rather than a sink of atmospheric methane (Fig. 12), as most values of methane concentrations at 10 m exceed those for equilibrium between ocean water and atmosphere. Methane concentrations and associated flux rates are highest close to the Bangladesh shelf area. They reach up to 28 kg km^{-2} yr^{-1}. Flux rates tend to decrease with increasing distance from the shelf, and approach near-equilibrium values close to the Equator.

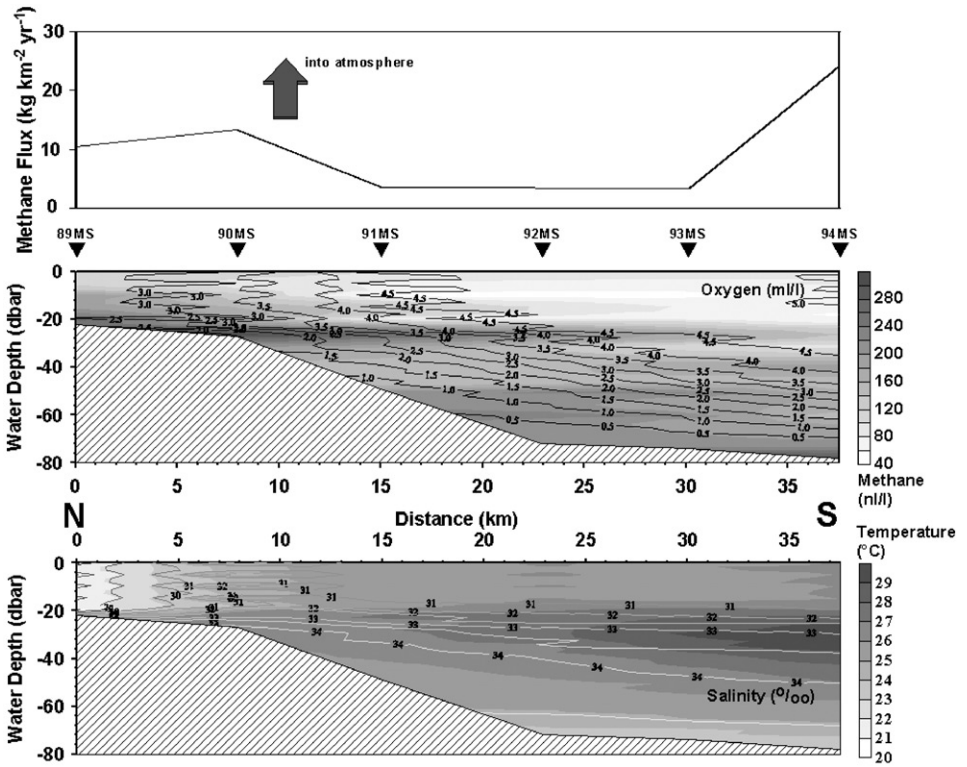

Fig. 14. Methane and oxygen concentrations, water temperatures and salinity of the eastern shelf of Bangladesh (N–S profile) and calculated methane flux rates (Profile 4).

4.3. Region 3: Bangladesh shelf and "Swatch of No Ground

Three short sections were occupied on the continental shelf of Bangladesh, one of which included five stations the northern part of the "Swatch of no Ground" down to a water depth of 600 m (Fig. 2, and Figs. 13–15; Profile 3 to Profile 5). As observed at two sections of the eastern shelf, surface currents were weak and variable in direction, apparently tidally dominated. The distributions of temperature, salinity and oxygen along the eastern shelf sections show the strong stratification on Profile 3 and 4 due to river run-off (Figs. 13 and 14). The waters were muddy and carried high amounts of suspended sediments. The oxygen is consumed fairly rapidly and oxygen minimum is reached at 60 m water depth (Figs. 13 and 14), most likely due to high inputs of degradable organic matter that serves as substrate for oxidizing bacteria.

Methane anomalies (up to 280 nl/l) of the N–S profile (Profile 4) are associated with the salinity and temperature jump at 20 m depth in oxygen-rich waters (Fig. 14). A second maximum occurs between 50 and 75 m below the temperature anomaly (20–50 m) in more oxygen-deficient waters.

The likely source of the methane in the surface water is methanogenic bacteria associated with the decay of organic debris or living as symbionts in the guts of zooplankton. The stratification could have lead to an accumulation effect at 20 m for settling organic particles due to the density changes and associated reduced settling velocities, thus explaining the methane anomaly at this water depth. The elevated methane concentrations below 50 m could be associated with in situ bacterial activity.

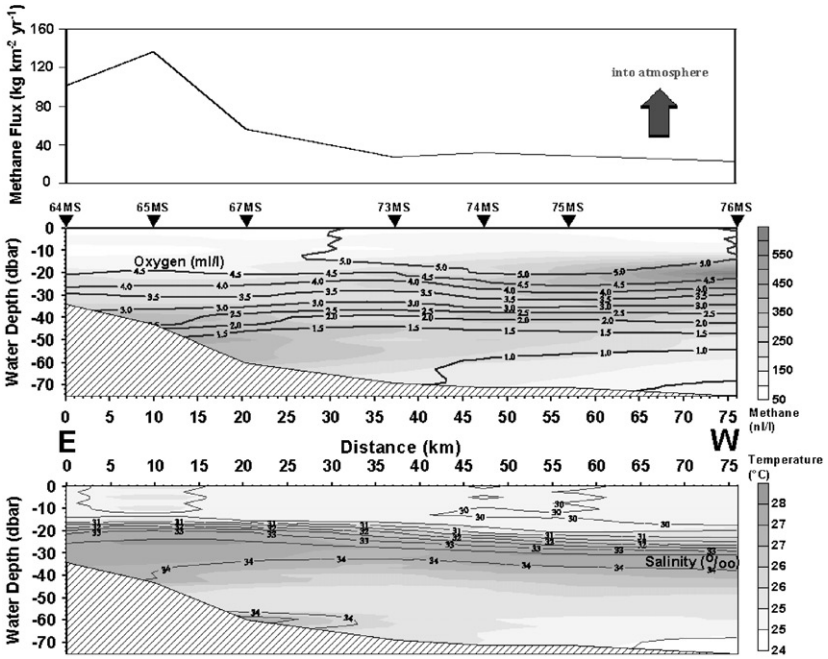

Fig. 15. Methane concentrations and water temperatures of the "Swatch of no Ground" (shelf of Bangladesh) and calculated methane flux rates (Profile 5).

Calculated methane fluxes of the Bengal Shelf are higher than in open-ocean areas, reaching values of up to 145 kg km^{-2} yr^{-1} (Fig. 13; Profile 3). The "Swatch of no Ground" (Profile 5) was filled with water masses from offshore and did not show any evidence for sinking freshwater from the Ganges and Brahmaputra Rivers. However, methane concentrations in the surface waters reached anomalous values of up to 880 nl/l (Fig. 15, Profile 5).

Flux rates of methane are higher than those offshore and reach up to 90 kg km^{-2} yr^{-1} on the shelf. However, at the two southernmost stations near-equilibrium conditions between water surface and atmosphere are reached.

5. Conclusions

- During the NE monsoon in January 1994 methane concentrations were clearly associated with the different water masses observed south of Sri Lanka. A 650-km-long profile from the Sri Lankan coast to the Equator revealed peak concentrations of 105 nl/l below 45 m water depth.
- Surface waters of the Bay of Bengal contained up to 800 nl/l of methane on the shelf close to the Ganges/Brahmaputra mouth. Methane concentrations of the surface waters are related to bacterial methanogenesis and bacterial oxidation as indicated by carbon isotope ratios of methane. This methane only partly contributes to the atmospheric methane concentrations, especially on the shelf of Bangladesh close to the Ganges/Brahmaputra mouth with flux rates of 145 kg km^{-2} year^{-1}. Large sections of the profiles, however, showed near-equilibrium conditions and even undersaturation of methane with respect to the atmosphere. Undersaturated areas presumably act as a methane sinks.
- Methane anomalies at 700 and 2100 m water depth on the continental slope off Bangladesh are related to gases likely emanating from the sediments, as indicated by seismic data. However, the deep methane anomalies do not exchange with the surface waters, and are not a source for atmospheric methane.

Acknowledgements

The authors thank D. Laszinski for the analyses of carbon isotope ratios of methane. The work was funded by the German Ministry of Education and Research through grants BMFT 03G 0093 A.

References

Atkinson, L.P., Richards, F.A., 1967. Deep-Sea Research II 14, 673–684.

Bange, H.W., Bartell, U.H., Rapsomanikis, S., Andreae, M.O., 1994. Methane in the baltic and North Seas and a reassessment of the marine emissions of methane. Global Biogeochemical Cycles 8 (4), 465–480.

Bange, H.W., Ramesh, R., Rapsomanikis, S., Andreae, M.O., 1998a. Methane in surface waters of the Arabian Sea. Geophysical Research Letters 25 (19), 3547–3550.

Bange, H.W., Breves, W., Mitzka, T., Lendt, R., Petuhov, K., Hupe, A., Rapsomanikis, S., Andreae, M.O., Reuter, R., Zeitschel, B., Ittekkot, V., 1998b. The surface distribution of nutrients, chlorophyll, and trace gases (CO_2, N_2O, CH_4) in the upwelling area of the northwestern Arabian Sea during the SW monsoon. Seventh national JGOFS-Workshop 1998, Bremen, pp. 8–9.

Chappellaz, J.A., 1990. Etude du methane atmospherique au cours du dernier cycle climatique a partir d l'analyse de l'air piege dans la glace antarctique. Ph.D. Thesis, University of Grenoble, 214pp.

Chappellaz, J.A., Barnola, J.M., Raynaud, D., Korotkevich, Y.S., Lorius, C., 1990. Ice-core record of atmospheric methane over the past 160,000 years. Nature 345, 127–131.

Chappellaz, J., Blunier, T., Raynaud, D., Barnola, J.M., Schwander, J., Stauffer, B., 1993. Synchronous changes in atmospheric CH_4 and Greenland climate between 40 and 8 kyrbp. Nature 366, 443–445.

Chappellaz, J.A., Brook, E.J., Blunier, T., Malaizé, B., 1997. CH_4 and $\delta^{18}O$ of O_2 records from Antarctic and Greenland ice: a clue for stratigraphic disturbance in the bottom part of the Greenland Ice Core Project and the Greenland Ice Sheet Project 2 ice cores. Journal of Geophysical Research 102, 26547–26557.

Conrad, R., Seiler, W., 1988. Methane and hydrogen in sea water (Atlantic Ocean). Deep-Sea Research II 35, 1903–1917.

Crutzen, P.J., 1991. Methane's sinks and sources. Nature 350, 380–381.

Dlugokencky, E.J., Masarie, K.A., Lang, P.M., Tans, P.P., 1998. Continuing decline in the growth rate of the atmospheric methane burden. Nature 393, 447–450.

Ericksson III, D.J., 1993. A stability dependent theory for air-sea gas exchange. Journal of Geophysical Research 98, 8471–8488.

Faber, E., Gerling, P., Berner, U., Sohns, E., 1994. Methane in ocean waters: concentrations and carbon isotope variability at East Pacific Rise and in the Arabian Sea. Environmental Monitoring and Assessment 31, 139–144.

Faber, E., Stahl, W.J., Berner, U., Gerling, P., Hollerbach, A., 1995. Methane in sediments, waters and in the atmosphere. Geotechnica 1995, 86–87.

Faber, E., Botz, R., Poggenburg, J., Schmitt, M., Stoffers, P., 1998. Methane in Red Sea brine waters. Organic Geochemistry 29 (1–3), 363–379.

Graedel, T.E., Crutzen, P.J., 1993. Atmospheric Change. An Earth System Perspective. Freeman and Company, New York, 446pp.

Heimann, M., 1997. Modellierung von klimarelevanten Stofffflüssen. VDI Berichte 1330, 61–68.

Hein, R., Crutzen, P.J., Heimann, M., 1997. An inverse modeling approach to investigate the global atmospheric methane cycle. Global Biogeochemical Cycles 11, 43–76.

Houghton, J.T., Jenkins, G.J., Ephraums, J.J., 1990. Climate Change. The IPCC Assessment. Cambridge University Press, Cambridge, pp. 18–22.

Karl, D.M., Tilbrook, B.D., 1994. Production and transport of methane in oceanic particulate organic matter. Nature 368, 732–734.

Liss, P.S., Merlivat, L., 1986. Air–sea exchange rates: introduction and synthesis. In: Buat-Ménard (Ed.), The Role of Air–sea Exchange in Geochemical Cycling. D. Reidel, New York, pp. 113–127

Michaelis, W., Faber, E., Plüger, W., Galimov, E., Keller, M., Paetsch, H., Boddem, J., Beckmann, W., et al., 1993. HYGAPE, Hydrothermale Gas und Partikel Exhalationen im Bereich des Ostpazifischen Rückens bei 21°S, SO80B. Zwischenbericht für das Forschungsprojekt 03R 420 B, Universität Hamburg, Institut für Biogeochemie und Meereschemie, Hamburg, August 1993, p. 178.

Oremland, R.S. (Ed.), 1993. Biogeochemistry of global change radioactively active face gases. Selected papers from the Tenth International Symposium on Environmental Biochemistry. San Francisco, August 19–24, 1991, 879pp, Chapman & Hall, NY.

Owens, N.J.P., Law, C.S., Mantoura, R.F.C., Burkill, P.H., Llewellyn, C.A., 1991. Methane flux to the atmosphere from the Arabian Sea. Nature 354, 293–296.

Rasmussen, R., Khalil, M.A.K., 1981. Atmospheric methane (CH_4): trends and seasonal cycles. Journal of Geophysical Research 86, 9826–9832.

Raynaud, D., Chappellaz, J.A., Barnola, J.M., Korotkevich, Y.S., Lorius, C., 1988. Climatic and CH_4 cycle implications of glacial–interglacial CH_4 change in the Vostok ice core. Nature 333, 655–657.

Schmitt, M., Faber, E., Botz, R., Stoffers, P., 1991. Extraction of methane from seawater using ultrasonic degassing. Analytical Chemistry 63 (5), 529–532.

Scranton, M.I., Brewer, P.G., 1977. Occurrence of methane in the near-surface waters of the western subtropical North-Atlantic. Deep-Sea Research II 24, 127–138.

Scranton, M.I., Farrington, J.W., 1977. Methane production in the waters of Walvis Bay. Journal of Geophysical Research 82, 4947–4953.

Suess, E., Bohrmann, G., Huene, R.V., Linke, P., Wallmann, K., Lammers, S., Sahling, H., Winckler, G., Lutz, R.A, Orange, D., 1998. Fluid venting in the Aleutian subduction zone. Journal of Geophysical Research 103 (B2), 2597–2614.

Ward, B.B., Kilpatrick, K.A., Novelli, P.C., Scranton, M.I., 1987. Methane oxidation and methane fluxes in the ocean surface layer and deep anoxic waters. Nature 327, 226–229.

Wanninkhof, R., 1992. Relationship between wind speed and gas exchange over the ocean. Journal of Geophysical Research 97 (C5), 7373–7382.

Welhan, J.A., 1988. Origins of methane in hydrothermal systems. Chemical Geolology 71, 183–198.

Whiticar, M.J., Faber, E., 1986. Methane oxidation in sediment and water column environments—Isotope evidence. In: Leythaeuser, D., Rullkötter, J. (Eds.), Advances in Organic Geochemistry, vol. 1985, pp. 759–768.

Whiticar, M.J., Faber, E., Schoell, M., 1986. Biogenic methane formation in marine and freshwater environments: CO_2 reduction vs. acetate fermentation - isotopic evidence. Geochimica et Cosmochimica Acta 50, 693–709.

Wiesenburg, D.A., Guinasso Jr., N.L., 1979. Equilibrium solubilities of methane, carbon monoxide, and hydrogen in water and sea water. Journal of Chemical and Engineering Data 24 (4), 356–360.

Wyrtki, K., 1973. Physical oceanography of the Indian Ocean. In: Zeitzschel, B. (Ed.), The Biology of the Indian Ocean. Springer, Berlin, pp. 18–36.